scientific reports

Check for updates

OPEN

Modeling a biofluid-derived extracellular vesicle surface signature to differentiate pediatric idiopathic nephrotic syndrome clinical subgroups

Giulia Cricri[1,2], Andrea Gobbini[3], Stefania Bruno[4], Linda Bellucci[1,2], Sarah Tassinari[5], Federico Caicci[6], Chiara Tamburello[2], Teresa Nittoli[2], Irene Paraboschi[7], Alfredo Berrettini[7], Renata Grifantini[3], Benedetta Bussolati[4], William Morello[2], Giovanni Montini[1,2,8,9] & Federica Collino[1,2,8,9]✉

Idiopathic Nephrotic Syndrome (INS) is a common childhood glomerular disease requiring intense immunosuppressive drug treatments. Prediction of treatment response and the occurrence of relapses remains challenging. Biofluid-derived extracellular vesicles (EVs) may serve as novel liquid biopsies for INS classification and monitoring. Our cohort was composed of 105 INS children at different clinical time points (onset, relapse, and persistent proteinuria, remission, respectively), and 19 healthy controls. The expression of 37 surface EV surface markers was evaluated by flow cytometry in serum ($n = 83$) and urine ($n = 74$) from INS children (mean age = 10.1, 58% males) at different time points. Urine EVs ($n = 7$) and serum EVs ($n = 11$) from age-matched healthy children (mean age = 7.8, 94% males) were also analyzed. Tetraspanin expression in urine EVs was enhanced during active disease phase in respect to the remission group and positively correlates with proteinuria levels. Unsupervised clustering analysis identified an INS signature of 8 markers related to immunity and angiogenesis/adhesion processes. The CD41b, CD29, and CD105 showed the best diagnostic scores separating the INS active phase from the healthy condition. Interestingly, combining urinary and serum EV markers from the same patient improved the precision of clinical staging separation. Three urinary biomarkers (CD19, CD44, and CD8) were able to classify INS based on steroid sensitivity. Biofluid EVs offer a non-invasive tool for INS clinical subclassification and "personalized" interventions.

Keywords Idiopathic nephrotic syndrome, Extracellular vesicles, Protein biomarkers, Steroid resistance

Idiopathic Nephrotic Syndrome (INS) is the most common form of glomerular disease in childhood, characterized by massive proteinuria, hypoalbuminemia, hyperlipidemia, and tissue edema[1]. The biological mechanisms leading to INS are poorly defined, but an immunological dysfunction has been advocated[2].

The current INS therapy is based on oral corticosteroids, which leads to complete remission in up to 80% of children, classified as steroid-sensitive (SSNS). However, SSNS children experience multiple relapses or even steroid dependence for which long-term immunosuppressive steroid-sparing agents are indicated[3]. Patients unresponsive to steroids (SRNS) show the most severe form and the need for kidney replacement therapy in 50% if remission is not achieved[4]. Both SSNS and SRNS can experience multiple adverse effects secondary to the

[1]Laboratory of Translational Research in Paediatric Nephro-Urology, Fondazione IRCCS Ca' Granda-Ospedale Maggiore Policlinico, Milan, Italy. [2]Paediatric Nephrology, Dialysis and Transplant Unit, Fondazione IRCCS Ca' Granda-Ospedale Maggiore Policlinico, Milan, Italy. [3]Istituto Nazionale Genetica Molecolare (INGM), Istituto Nazionale Genetica Molecolare Romeo ed Enrica Invernizzi, Milan, Italy. [4]Department of Medical Sciences, University of Turin, Turin, Italy. [5]Department of Molecular Biotechnology and Health Sciences, University of Turin, Turin, Italy. [6]Department of Biology, University of Padova, Padua, Italy. [7]Pediatric Urology Unit, Fondazione IRCCS Ca' Granda-Ospedale Maggiore Policlinico, Milan, Italy. [8]Department of Clinical Sciences and Community Health, University of Milano, Milan, Italy. [9]These authors contributed equally: Giovanni Montini and Federica Collino. ✉email: federica.collino@unimi.it

immunosuppressive treatment[5,6]. There is therefore a major medical need to find early biomarkers to allow for a more precise selection and duration of the treatment and to characterize the INS subgroups for clinical studies.

Extracellular vesicles (EVs) are nanosized particles naturally released by almost all cell types[7,8] and are easily found in many body fluids. EVs can carry selective surface markers inherited from their parent cells[9], mirroring the functional state of the originating tissue. EVs contain lipids, proteins, and different forms of nucleic acids that are actively released from the cells from which they are derived[10]. Extensive investigation has been conducted on the wide array of molecules that can be enclosed within EVs, owing to their substantial relevance as biomarkers for various diseases[11].

Urinary EVs (uEVs) originate mainly from the kidney and urinary tract cells[12] and can be a source of important urinary biomarkers reflecting the molecular processes activated by kidney diseases[13]. uEVs have been used for an early diagnosis of chronic kidney disease (CKD)[14], polycystic kidney disease[15], active glomerulonephritis[16], and tubulopathies[17]. Moreover, uEVs can be secreted by kidney-resident immune cells, acting as biomarkers of immune activation and tissue remodelling[18]. When the glomerular and tubular basement membranes are disrupted, uEVs may also derive from the bloodstream representing other body compartments[19].

This study aimed to identify the expression signature of uEVs reflecting the different forms of INS in childhood and the possible response to the treatment before the start of therapy.

Methods

Patient recruitment strategy and clinical data

Children with INS (first episode below 18 years old) were enrolled at the Pediatric Nephrology, Dialysis and Transplant Unit (Fondazione IRCCS Ca' Granda Ospedale Maggiore Policlinico of Milano) in the period January 2022 to February 2023. A control group of age-matched children, with no kidney-related or immunological disease, was included in the study (CTRL). This study was conducted according to the principles expressed in the Declaration of Helsinki. Approve to the study was obtained by the IRCCS Ca' Granda Institutional Review Board (ID 2633, INSiDe protocol). An informed consensus was obtained for all the participants enrolled in the study. Patients were treated with standard therapy with oral prednisone and classified according to the international guidelines as SSNS or SRNS[3,20]. Demographic data, current therapies, and responses to ongoing therapy were collected. Routine clinical and biochemical parameters were measured according to the clinical practice. Proteinuria was defined as urine protein/creatinine ratio (uPr/uCr) $\geq$ 0.2 mg/mg (mild proteinuria, 0.21–1.99 mg/mg and nephrotic range proteinuria, $>$ 2 mg/mg). eGFR was calculated using the modified Schwartz formula.

Study sample collection

Blood and urine were collected from children with INS and an age-matched control group (CTRL). Urine samples were processed within 6 h (h) of collection according to established protocols[21,22]. Serum was obtained by activating the coagulation cascade from peripheral whole blood, followed by centrifugation at 3000 g for 20 min to remove corpuscular components. Aliquots of serum and urine were stored at -80 °C until use.

Urine and serum EVs characterization

Unpurified extracellular vesicles (EVs) from urine and serum samples were used. Dedicated urine samples underwent ultracentrifugation at 100.000 g for 2 h at 4 °C for EV isolation (Beckman Coulter, OPTIMA XPN-90 Ultracentrifuge, Rotor Type 70-Ti, Brea, CA). EVs were then resuspended in PBS (Sigma-Aldrich) and freshly used or in 1% dimethyl sulfoxide (DMSO) (Sigma-Aldrich) and stored at − 80 °C. Nanoparticle tracking analysis (NTA) was conducted on unpurified EVs using the Nanosight NS300 and analyzed as previously reported[23]. uCr was used as a normalization variable for particles number quantification in urines from both healthy subjects and patients with INS. Characterization involved Transmission Electron Microscopy, Super-Resolution Microscopy, and Exoview analysis. Detailed procedures are reported in the Supplementary material (Supplementary technical method description).

Cytofluorimetric analysis of EVs

100 µL of unpurified urine EVs (uEVs) and 1×10^{10} of unpurified serum EVs (sEVs) were analyzed using a MACSPlex human Exosome kit (Miltenyi Biotec) according to the manufacturer's instructions. For uEVs, surface marker median fluorescence intensity (MFI) was normalized against spot urine Creatinine (uCr, g/L) to account for inter-patient EV variations based on the daily water intake. Flow cytometry was conducted on Cytoflex using CytExpert Software (Beckman Coulter, Brea, CA, USA), and data were analyzed with Flowjo software (Tree Star, Inc. Ashland, OR, USA). Raw data were reported in the Supplementary material (Supplementary cytofluorimetric data).

Statistics

Analysis was performed using RStudio (R v4.0.3) or Prism with GraphPad v9.0 (GraphPad Software, USA). Normalized cytofluorimetric signals were log-transformed for urine and serum markers. Transformed markers were used both for multivariate and univariate analysis.

Principal components analysis (PCA) and clustering were done using FactoMineR (v2.4) and Complex Heatmap (v2.6.2), respectively. Two-sided Student's or Mann-Whitney tests for pairwise comparisons and one-way ANOVA with Tukey's post hoc tests or Kruskal-Wallis's test with Dunn's post hoc for multiple comparisons were selected based on data distribution.

Correlation with biochemical variables was assessed using Pearson or Spearman coefficients.

Marker frequency (% protein positivity/total samples analyzed) among patient groups was determined with a < 50% or > 50% threshold as previously reported[24]. The classification performance of both single markers and their combinations was evaluated using combiROC (v0.2.3) (sensitivity ≥ 40, specificity ≥ 70, AUC).

Odds ratios (ORs) were calculated with univariate logistic regression (OR > 1 indicates increased likelihood of association with SRNS appearance, OR < 1 indicates decreased association). Significance was set at $P < 0.05$.

Results

Demographic and clinical variables

Table 1 summarizes the clinical and biochemical characteristics of the INS study cohort ($n = 105$, 58% males) and healthy controls (CTRL) ($n = 19$, 94% males). The study cohort includes SSNS ($n = 80$) and SRNS ($n = 25$).

The INS population was then subdivided into five groups: Group 1 SSNS patients at the onset of the disease ($n = 17$, SSNS Onset); -Group 2 SSNS at relapse (SSNS Rel, $n = 37$); -Group 3 SRNS patients with persistent proteinuria (above 0.5 mg/mg) (SRNS, $n = 17$); -Group 4 SSNS in remission (SSNS Rem, $n = 26$); -Group 5 SRNS patients who achieved complete response to second-line treatments (SRNS Rem, $n = 8$). A control group of age-matched children, with no kidney-related or immunological disease, was included in the study (CTRL). In selected experiments, children in groups 1, 2, and 3 were selected as patients with active INS ($n = 71$), while children in groups 4 and 5 were in the remission phase of the disease (inactive INS, $n = 34$). In our cohort, the age was homogenously distributed with a median of 8.5 years (IQR: 4–13) in SSNS and 6 years (IQR: 2–11) in

Parameters	Healthy children CTRL	Active INS disease ($n = 71$)	SSNS		SRNS	Inactive INS disease ($n = 34$)	SSNS	SRNS	p value
	($n = 19$)		Onset ($n = 17$)	Rel ($n = 37$)	($n = 17$)		Rem ($n = 26$)	Rem ($n = 8$)	
Demographic and clinical characteristics									
Sex, n (%)									
Male	18, (94.7)	43, (60.6)	11, (64.7)	24, (64.9)	8, (47.1)	18, (52.9)	13, (50)	5, (62.5)	
Female	1, (5.3)	28, (39.4)	6, (35.3)	13, (35.1)	9, (52.9)	16, (47.1)	13, (50)	3, (37.5)	
Age (yr), median (IQR)	6 (2–11)	9, (4–15)	4 (3–13)	8 (5–12)	15 (12-18.5) **a**, **b**, **c**	11, (8-14.25)	11 (6-13.25)	15 (8.25–17.75)	**a**, **c** $p < 0.01$ **b** $p < 0.001$
Age at onset (yr), median (IQR)	N/A	4, (3–12)	4 (3–13)	4 (2–5)	9 (4–15) **c**, **d**	5, (3–8)	4 (2.37–7.25)	7 (5.25–12.50)	**c** $p < 0.01$ **d** $p < 0.05$
Drugs treatment at the time of collection, n (%)									
Immunosuppressants	0, (0)	25, (35.2)	0, (0)	14, (37.8)	11, (64.7)	30, (88.2)	24, (92.3)	6, (75)	
Others	0, (0)	4, (5.6)	0, (0)	0, (0)	4, (23.5)	0, (0)	0, (0)	0, (0)	
NT	19, (100)	42, (59.1)	17, (100)	23, (62.2)	2, (11.8)	4, (11.8)	2, (7.70)	2, (25)	
Biochemical parameters									
Protein-to-creatinine ratio, median (IQR)	N/A	5.85, (1.86–8.7) **f**	8.5 (4.96–9.27) **d**, **e**	3.7 (1.60–8.52) **d**, **e**	2.68 (0.96–8.78) **d**	0.15, (0.12–0.18)	0.14 (0.11–0.16)	0.31 (0.19–0.63)	**d**, **f** $p < 0.001$ **e** $p < 0.05$
Urine creatinine (g/L), median (IQR)	0.77 (0.42–1.23)	0.99, (0.59–1.6)	0.8 (0.47–1.56)	1.0 (0.63–1.64)	0.98 (0.57–1.88)	1.19, (0.8–1.54)	1.05 (0.57–1.48)	1.49 (1.02–1.80)	
Serum creatinine (mg/dL), median (IQR)	0.46 (0.29–0.56)	0.45, (0.31–0.68)	0.31 (0.26–0.50) **e**	0.40 (0.32–0.59)	0.84 (0.56–1.06) **a**, **b**, **c**	0.52, (0.46–0.62)	0.51 (0.43–0.57)	0.67 (0.47–0.95)	**a** $p < 0.01$ **b**, **c** $p < 0.001$ **e** $p < 0.05$
eGFR (mL/min), median (IQR)	107 (86–132)	118, (91–145)	138 (101.5-163.5)	122 (106.8-149.8)	74 (58.50–106) **b**, **c**, **d**	115, (93–126)	117 (96.45–126.8)	99 (78-119.5)	**b**, **c** $p < 0.001$ **d** $p < 0.05$
Immunoglobulins (mg/dL), median (IQR)									
IgG	N/A	383, (148–618) **f**	150 (93–230) **c**, **d**, **e**	487 (365.5-719.5)	571 (186.5–679)	695, (500.3–919)	695 (465-849.3)	763 (644.8–1128)	**c** $p < 0.01$ **d**, **e**,**f** $p < 0.001$
IgM	N/A	127, (96.3–184) **f**	121 (100-201.5) **d**	127 (72–163)	162 (114.8–194) **d**	66, (38–110)	57 (37.5–112)	82 (58.25–118.8)	**d** $p < 0.05$ **f** $p < 0.001$
IgA	N/A	92, (72.3-138.8)	103 (57-168.5)	83 (59–129)	92 (69-192.5)	98, (46–151)	71 (31.5–110)	143 (95.50–234)	

Table 1. Clinical characteristics of the enrolled patients at the time of collection. Immunosuppressant drugs: prednisone, mycophenolate, tacrolimus, Others: ramipril. Values vs. **(a)** CTRL, **(b)** SSNS onset, **(c)** SSNS Rel **(d)**, SSNS Rem **(e)**, SRNS Rem, and **(f)** Inactive INS. *NT* not treated, *IQR* interquartile range, *N/A* not applicable.

CTRL, while SRNS patients had a higher median age of 15 years (IQR: 10–18). eGFR was reduced (74 mL/min) in SRNS compared to SSNS subgroups (138 and 122 mL/min for SSNS Onset and SSNS Rel, respectively). Serum IgG and IgM levels varied according to disease phase[25], as expected.

Qualitative and quantitative evaluation of urine EVs in INS

EVs isolated from the urine of INS children (uEVs) exhibited a heterogeneous size and preserved membranes, confirmed by TEM analysis (Fig. 1A). Super-resolution microscopy qualitative analysis revealed tetraspanin distribution on single vesicles in both CTRL and INS patients (Fig. 1B). Quantitative analysis showed significantly higher CD63 + and CD81 + uEVs in active INS (62,500 ± 23,300 and 65,700 ± 21,000 respectively, $P < 0.05$ and $P < 0.01$) compared to CTRL (22,100 ± 10,200, and 22,000 ± 9,600) and inactive INS (only for CD81, 28,800 ± 10,500, $P < 0.05$) (Fig. 1C). Capture separation revealed different co-expression patterns among tetraspanins (Fig. 1D), particularly significant for CD9/CD63 and CD81/CD63 in the active phase compared to CTRL ($P < 0.05$ and < 0.01, respectively). EVs co-expressing CD81/CD63 also showed a different distribution between the active and inactive INS stages ($P < 0.05$). Triple-positive uEVs were less abundant but significantly increased in the active phase when captured with CD9 ($P < 0.001$ vs. CTRL and $P < 0.01$ vs. inactive INS) and CD81 antibodies ($P < 0.05$ vs. both groups).

Correlations between uEVs/mL in both INS and CTRL urine and kidney function parameters (uCr, uPr/Cr, eGFR) were investigated (Fig. 2A). Spearman's analysis revealed a significant positive correlation between uEV numbers and uCr levels ($R = 0.29$, $P < 0.01$), as well as with the uPr/uCr ratio ($R = 0.22$, $P < 0.05$). uEV dimensions negatively correlated only with the uPr/uCr levels (R=-0.27, $P < 0.01$) (Fig. 2B). These associations persisted when INS patients were separated from controls (Additional File 1: Figure S1). In detail, we observed a significant positive correlation of uEV numbers with uCr levels ($R = 0.31$, $P < 0.01$) and with uPr/uCr ($R = 0.22$, $P < 0.05$) (Fig. S1A). uEV dimensions negatively correlated with both uCr (R=-0.22, $P < 0.05$) and uPr/uCr levels (R=-0.29, $P < 0.01$) (Fig. S1B). Separation based on gender, highlighted as the positive correlation with uCr and uPr/uCr was maintained only in the female group. The same was observed for the negative correlation between EV size distribution and uPr/uCr levels. NTA analysis (Fig. 2C) showed increased uEV numbers (uEVs/uCr) in SSNS Onset compared to CTRL ($P < 0.01$), and the other groups and clinical time-points ($P < 0.001$) whereas EV size distribution decreased only between SRNS and SSNS in remission ($P < 0.05$, SSNS Rem vs. SRNS Rem) (Fig. 2D). No gender-based differences were observed in uEV numbers and size in INS (Fig. 2C, D).

uEV surface marker characterization in different INS groups

uEV surface marker profile was evaluated by flow cytometry in seventy-four INS patients. CD9-CD63-CD81 EV expression positively correlated with uPr/uCr (Fig. 3A), with CD9 most significantly associated with the active state ($R = 0.54$, $P < 0.001$). Tetraspanin levels were higher in active INS compared to controls and inactive INS (CD9 and CD63 $P < 0.05$ vs. CTRL and $P < 0.001$ vs. inactive INS; CD81 $P < 0.001$ vs. inactive INS) (Fig. 3B).

Global EV-surface antigens distribution in each INS, analyzed through PCA, distinctly separated SSNS in relapse from onset and the SRNS group (Fig. 3C). Unsupervised hierarchical clustering confirmed the clustering of INS patients in the active phase (Fig. 3D). Marker frequency analysis revealed exclusive markers in INS children (CD25, CD20, CD11c, CD2, CD49e, CD62p, and CD42a) with higher frequencies during the active phase than during remission (Frequency > 50%). In the active INS phase, SRNS exhibited higher levels of adaptive immune-related proteins (CD4, CD8, CD19), monocyte markers (CD11c, CD2, CD1c), and adhesion molecules (CD49e, CD146) compared to the SSNS group (Fig. 3E).

Identification of uEV-associated markers to distinguish the active phase of INS disease

Nineteen core EV-surface markers were identified as potential discriminants between active and inactive INS (Fig. 4A), with eight effectively distinguishing the active phase from CTRL (Fig. 4A). Among them, the three markers that achieved the best discrimination were CD41b, CD105, and CD29 with an AUC > 0.88 (Fig. 4B). These 19 core markers, excluding CD24, CD1c, CD11c, CD25, and CD40, and with the addition of CD19 and CD69 molecules, exhibited a significant positive correlation with proteinuria levels in INS children (Table 2), suggesting an association between kidney damage and uEVs of distinct cellular origin.

Seven markers effectively separated SSNS at the onset from CTRL (Supplementary material; Table S1), with CD41b achieving the highest performance (AUC > 0.9). The same cluster of markers except for CD20 and CD42a, but including CD326, CD9, CD133, CD63, CD81, and CD24 differentiated between SSNS Rel and SSNS Rem groups (Supplementary material; Table S2), with CD29 showing the best AUC. When the SRNS group was analyzed, almost half of the markers were differentially expressed between patients with persistent proteinuria or in remission after second-line immunosuppressive treatments. Best AUC values were obtained for CD9, CD19, and CD146 (AUC: 1, 0.94, and 0.92, respectively) (Supplementary material, Table S3).

Identification of a candidate uEV panel to discriminate patient's sensitivity to the steroid therapy

uEVs from SSNS Rel and SRNS patients were compared to identify biomarkers that differentiated the two groups significantly. Markers encompassing both innate (CD11c, CD209, and CD1c) and adaptive immune responses (CD19, CD4, and CD8), along with those involved in angiogenesis/adhesion and stemness processes (CD31, CD44, CD146, and ROR1) were identified (Fig. 5A). CD146 emerged as a significant predictor for SRNS (Fig. 5B). However, the best separation between SRNS and SSNS Rel groups was achieved by the combination of CD19-CD44-CD8 (AUC = 0.87) (Fig. 5C; Table 3).

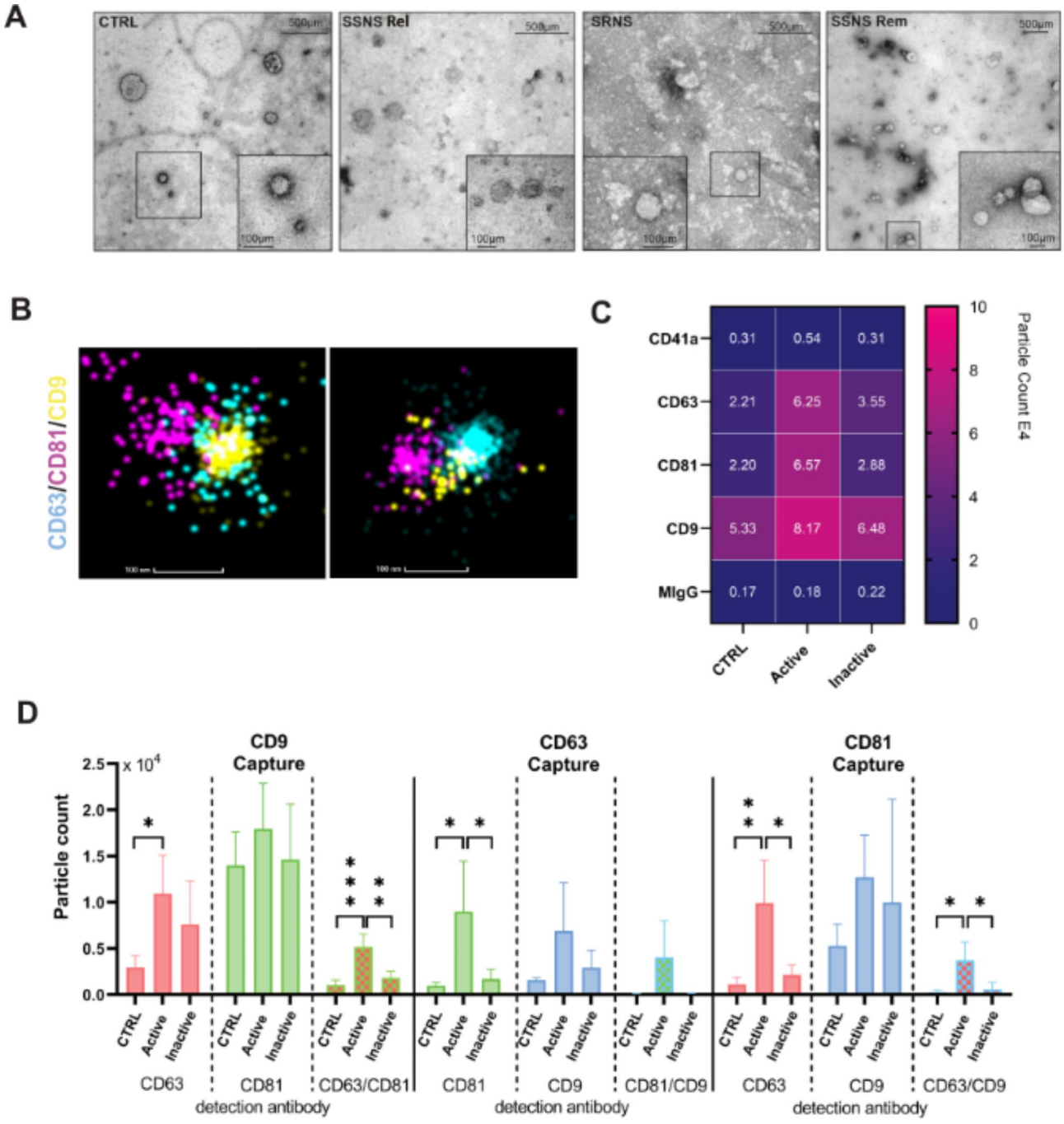

Fig. 1. Characterization of EVs released into the urine of INS children. (**A**) TEM analysis of purified EVs from urines of CTRL, SSNS Rel, SRNS, and SSNS Rem patients; representative low- and high-power field images (inset panel), showed heterogeneous EV population; scale bars = 500 µm and 100 µm. (**B**) Qualitative distribution visualization of tetraspanins in uEVs by Super-Resolution Microscopy (SRM); representative SRM images of CTRL (left panel) and INS uEVs (right panel) showing the expression of CD9 (yellow), CD63 (blue), and CD81 (purple). (**C**, **D**) High throughput fluorescence profiling of tetraspanins expression in single particles released into the urine of CTRL (n = 3), and INS patients both in the active (n = 6), and inactive phase of the disease (n = 4); (**C**) number of fluorescent particles expressing each tetraspanin compared to non-specific capture IgG (IgG) and (**D**) tetraspanins co-expression pattern determined by multiple detection antibodies on single tetraspanins capture spot (3 technical replicates representing 3 capture spots each were analyzed). *P < 0.05, **P < 0.01, and ***P < 0.001; One-way ANOVA with Tukey's post-test.

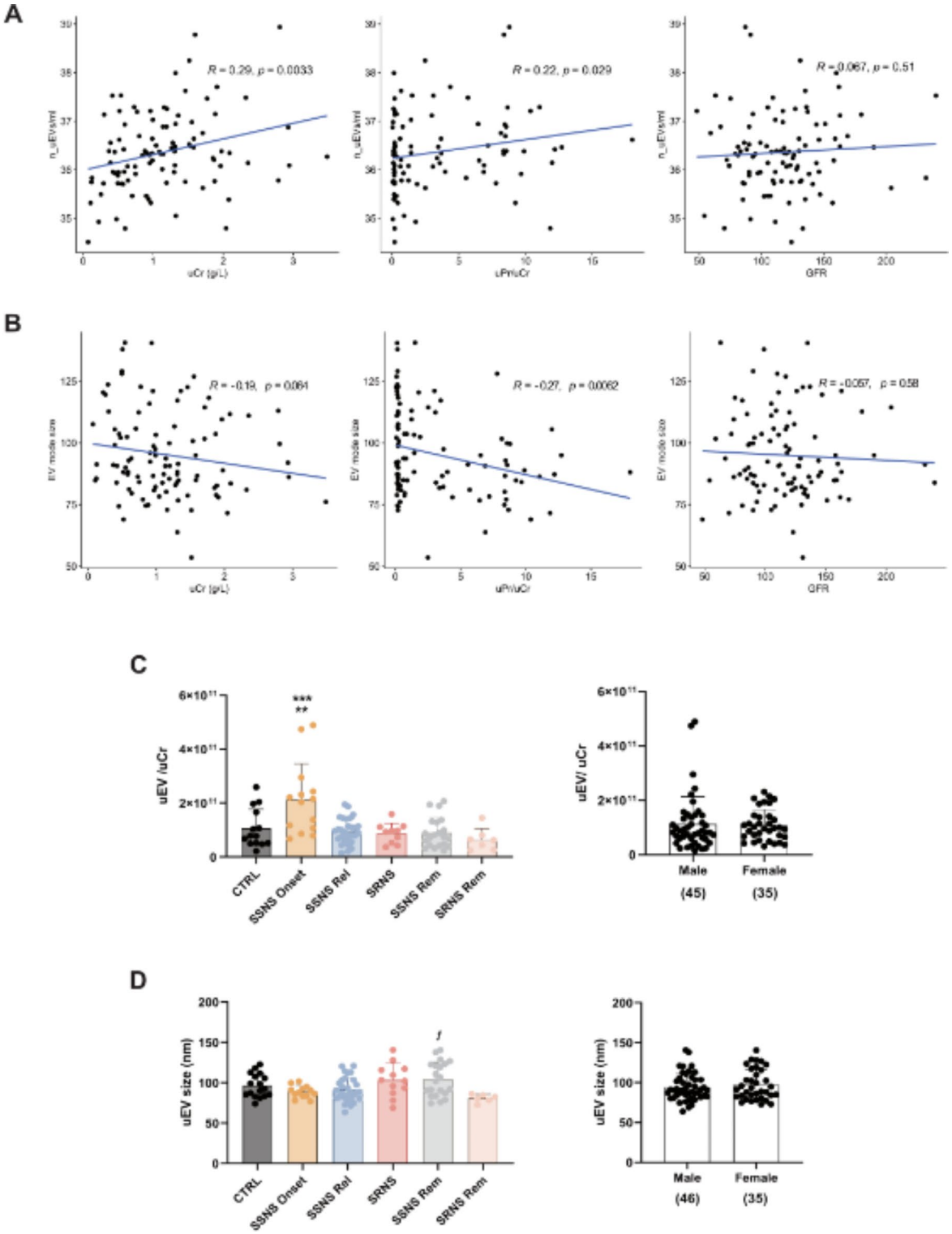

Fig. 2. Characterization of uEVs from CTRL and INS patients by NTA and correlation with renal function parameters. Correlations of uEV concentration (**A**) and size (**B**) with the renal function biochemical parameters (uCr, uPr/uCr, and eGFR) are reported. R = Spearman correlation coefficient. $P < 0.05$ has been considered statistically significant. Normalized uEVs concentration (number of particles/urine creatinine, uEV/ uCr) (**C**) and size distribution (mode) (**D**) in the INS group and CTRL are reported. Analysis of the number (**C**, right panel) and size (**D**, right panel) of uEVs between males and females in the INS cohort is also shown. Data are presented as means ± standard deviation (SD) of individual data points. **$P < 0.01$ vs. CTRL, ***$P < 0.001$ vs. SSNS Rel, SRNS, SSNS, and SRNS Rem; $ƒP < 0.05$, vs. SRNS Rem; One-way ANOVA with Tukey's post-test.

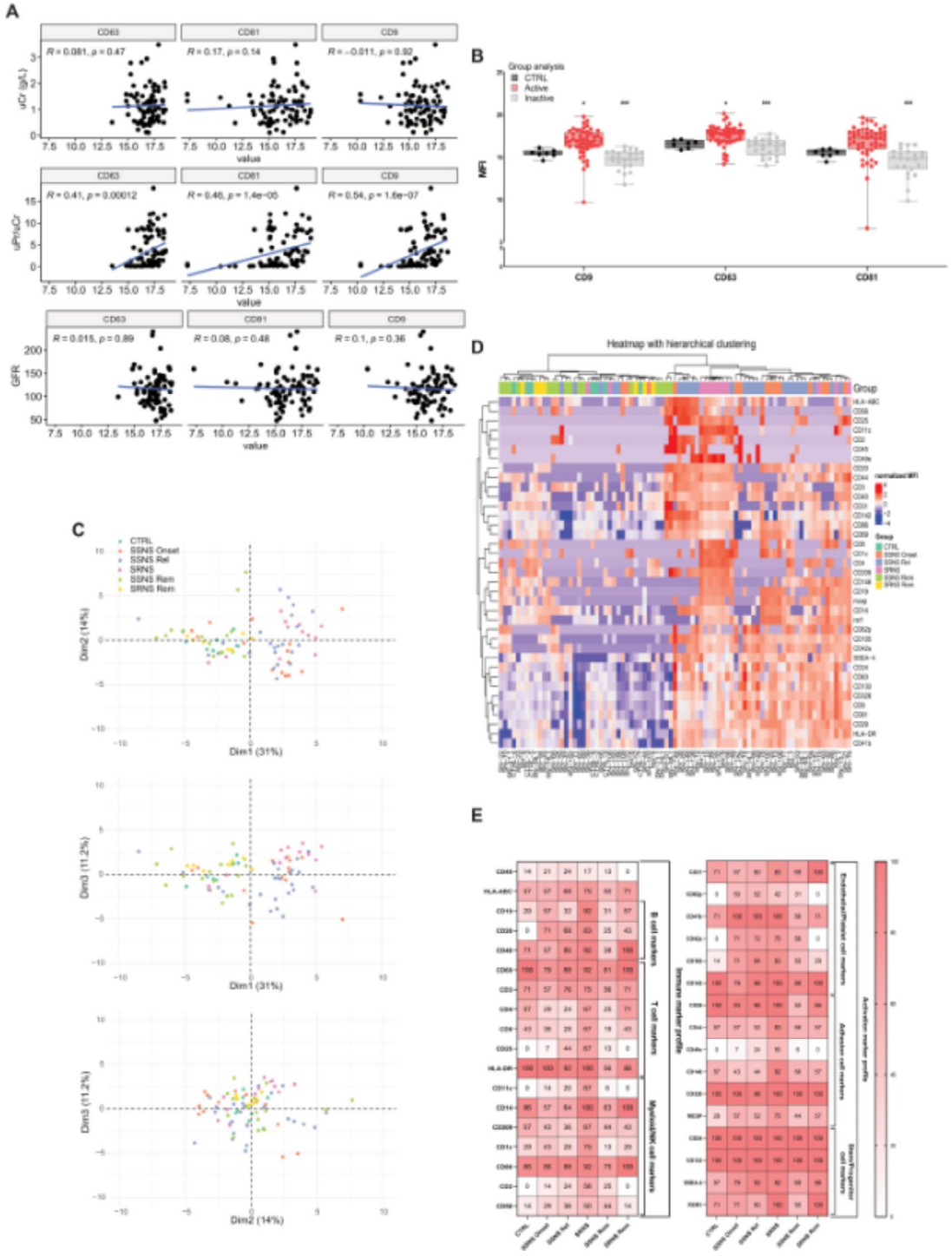

Fig. 3. Identification of urinary EV signature in INS children. (**A**) Spearman's correlation analysis between tetraspanins expression (Median Fluorescence Intensity, MFI on X axis) and biochemical parameters of renal function (uCr, uPr/uCr, eGFR); R = Spearman correlation coefficient, $P < 0.05$ has been considered statistically significant. (**B**) Flow cytometry characterization of tetraspanins in EVs from INS patients at different clinical time points, expressed as normalized MFI (MFI/ uCr) (CTRL n = 7, Active INS n = 51 and Inactive INS n = 23). *P < 0.05 vs. CTRL; ###P < 0.001 vs. Active INS; Kruskal-Wallis non-parametric with Dunn's post-test. (**C**) Principal component analysis (PCA) plots individuals' urine EVs protein content (dim1 vs. dim2, dim1 vs. dim3, dim2 vs. dim3). CTRL, active, and inactive INS patient groups were analyzed (each patient's subgroup is defined by color). (**D**) Heatmap analysis of uEV signature distribution detected by cytofluorimetric analysis in the analyzed cohort (z-score distribution for each protein). (**E**) The frequency distribution (%) of the 34 exosomal protein markers in INS patients and control children is indicated in each box. Darker red plots represent higher marker frequency.

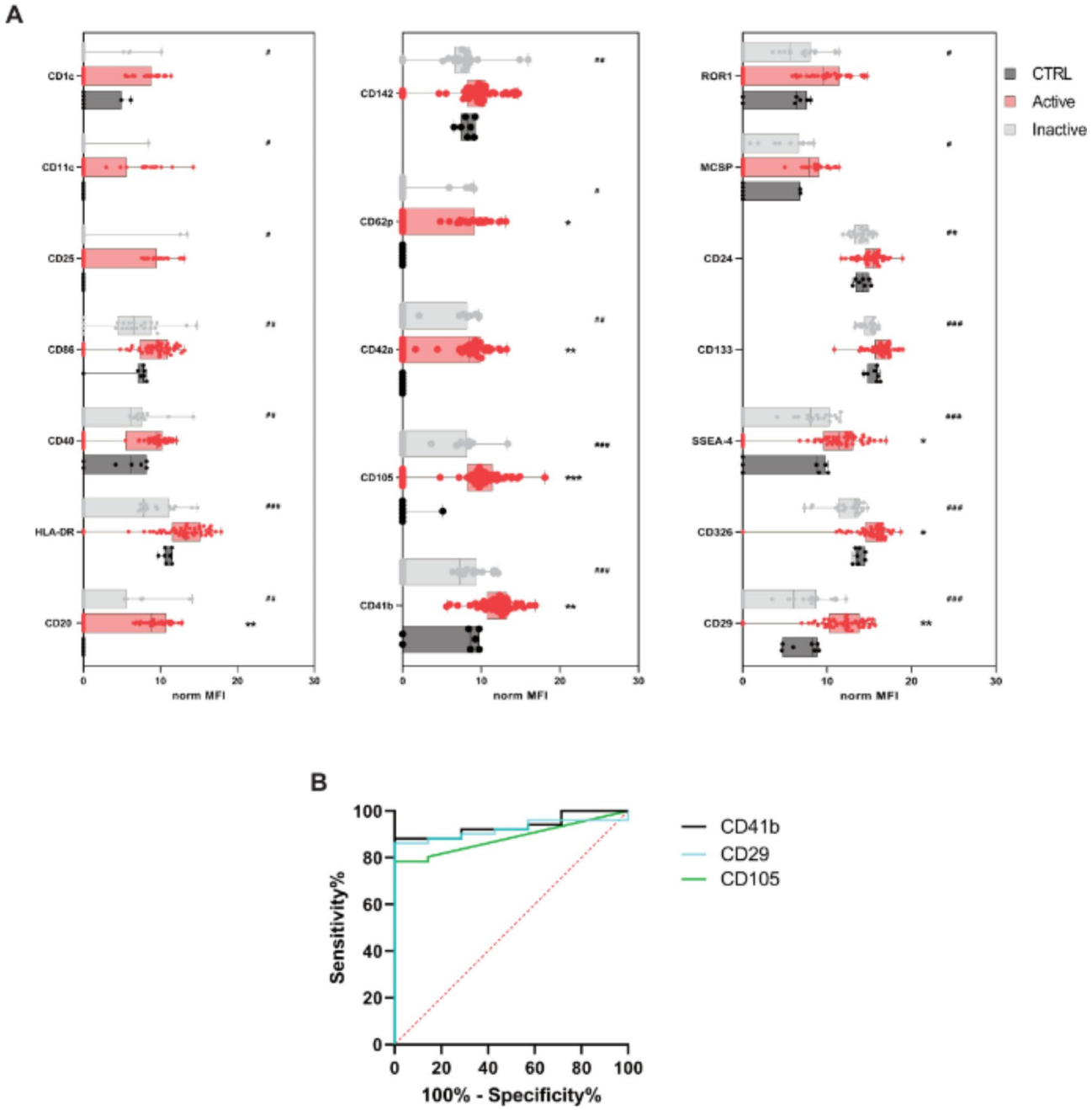

Fig. 4. Expression of uEV markers between INS at different clinical stages and pediatric controls. (**A**) Boxplots showing expression of a cluster of immune, platelets, and adhesion/progenitor cell markers in CTRL, and active or inactive INS. *P < 0.05, **<*0.01*, and ***<*0.001* vs. CTRL; #P < 0.05, ##<*0.01*, ###<*0.001* vs. active INS. Kruskal-Wallis non-parametric with Dunn's post-test. (**B**) ROC curve analysis of the performance of the CD41b, CD29, and CD105 markers, in separating the active INS group from CTRL.

Generation of INS expression signature using the serum and urinary EVs from the same patient

EVs enriched in the serum (sEVs) were also characterized in eighty-three INS patients. NTA analysis revealed significantly higher sEV numbers in SSNS at onset (7.87e11 ± 3.13e11 part/mL, $P < 0.01$) and relapse compared to CTRL (6.50e11 ± 2.92e11 part/mL vs. 3.79e11 ± 1.38e11, P < 0.05) (Fig. 6A). sEVs were also increased in SRNS with persistent proteinuria compared to CTRL (P < 0.001) and SSNS Rem (P < 0.05). No differences in sEV size were observed among groups or after gender-related INS separation (Fig. 6B). CD9 expression in sEVs decreased during the active phase compared to CTRL and inactive INS (P < 0.01 and < *0.05*, respectively) (Fig. 6C). Three markers on serum EV surfaces were identified as potential discriminants for active INS (not shown), with lower discriminating power compared to urine in distinguishing INS patients from controls. The combination of serum and urine markers from the same patient was able to reach a statistical correlation as observed in Fig. 6D,

Cellular Origin	Markers	*R*	*p*-value
Immune cell compartment	**CD19**	0.43	< 0.001
	CD20	0.38	< 0.001
	HLA-DR	0.62	< 0.001
	CD69	0.29	< 0.01
	CD86	0.26	< 0.05
Endothelial/platelet activation	**CD62p**	0.32	< 0.01
	CD41b	0.71	< 0.001
	CD42a	0.33	< 0.01
	CD105	0.44	< 0.001
	CD142	0.23	< 0.05
Adhesion cell activation	**CD29**	0.68	< 0.001
	CD326	0.59	< 0.001
	MCSP	0.32	< 0.01
Stem/Progenitor cell activation	**CD133**	0.43	< 0.001
	SSEA-4	0.48	< 0.001
	ROR1	0.44	< 0.001

Table 2. Urine-EV biomarkers and their correlation to pathological proteinuria. R = Spearman Correlation Coefficient. *P value* < 0.05 was considered significant.

with CD3 and CD29 exhibiting significant positive/negative relations in both matrices ($R = 0.25$, $P = 0.047$ and $R = -0.26$, $P = 0.039$, Pearson correlation) (Fig. 6D). Likewise, the combination of sCD146 and uCD29-uCD41b separated active INS patients from healthy children with higher sensitivity (SE ~ 1) compared to single markers; the combination of CD41b in serum and urine distinguished SSNS at onset from CTRL, and in SSNS, uCD326, and sCD8 effectively differentiated disease activity (Table 4).

Discussion

In the present study, we analyzed the surface antigen profile of urine and serum EVs in a cohort of pediatric INS patients, searching for new biomarkers for the accurate subclassification of INS sub-cohorts for clinical studies. Through the combination of a standardized surface proteomic analysis with a bioinformatic approach, a urine EV-based signature was generated, discriminating different forms of childhood INS compared with a cohort of paediatric controls. Urine-EV signature was mainly characterized by markers of endothelial/platelet and immune stimulation during proteinuria events. Conversely, the combination of serum and urine EVs was able to improve the separation between the different groups of childhood INS.

We found that at the onset of the disease, patients present more EVs in their urine compared to healthy children. This was in line with previous studies showing the association of EV abundance with different pathological conditions related to the kidney[26]. EV concentration can be influenced by age[27]. In our patient's cohort, the age was uniformly distributed among the different phases of the disease and comparable to the control group. The only form showing a different age distribution was the SRNS group classically characterized by a higher age of appearance of the disease[28]. However, no differences were highlighted in their EV number in respect to the SSNS. The number of uEVs also showed a positive correlation with proteinuria levels in the different INS groups.

The classical tetraspanin members were detectable in the urine EVs, with the highest expression observed from CD9, followed by CD81 and CD63 in proteinuric INS. When a co-expression pattern was investigated, double-positive CD63/CD81 vesicles were identified as the most enriched EVs in the INS active phase, with a significant reduction during the inactive phase. Interestingly, all the tetraspanins showed a stronger association with proteinuria level, where the highest correlation was achieved for CD9, displaying a direct relation between tetraspanins and early kidney disease.

We here, for the first time, characterized uEVs in INS patients, tracking their cellular sources using a standardized flow cytometric assay able to simultaneously analyze 37 different markers. A characteristic uEV protein electrophoresis profile was previously found able to discriminate INS from other non-glomerular kidney diseases[29]. Previous studies by Burrello et al. used the same cytofluorimetric technology to investigate the surface antigen profile of blood and urine EVs in ischemic brain injury[30] and rejection episodes associated with heart and kidney transplantation[23,31].

The uEV concentration can be dependent on the excretion/fusion EV rate and the overall urine concentration. Blijdorp et al. demonstrated that uEV concentration highly correlates with urine creatinine, potentially replacing the need for uEV quantification to normalize spot urines[32]. Indeed, urine creatinine levels are commonly used to normalize the excretion rate of different urinary analytes[33,34]. In our study, a positive correlation between the concentration of released EVs and urine creatinine was observed. Therefore, we employed the urinary creatinine measure to normalize the relative excretion rate of uEV proteins.

By applying hierarchical clustering on urinary EV markers, we revealed a superimposable pattern between INS children at the onset of the pathology and during relapse; however, these two groups exhibited a group of

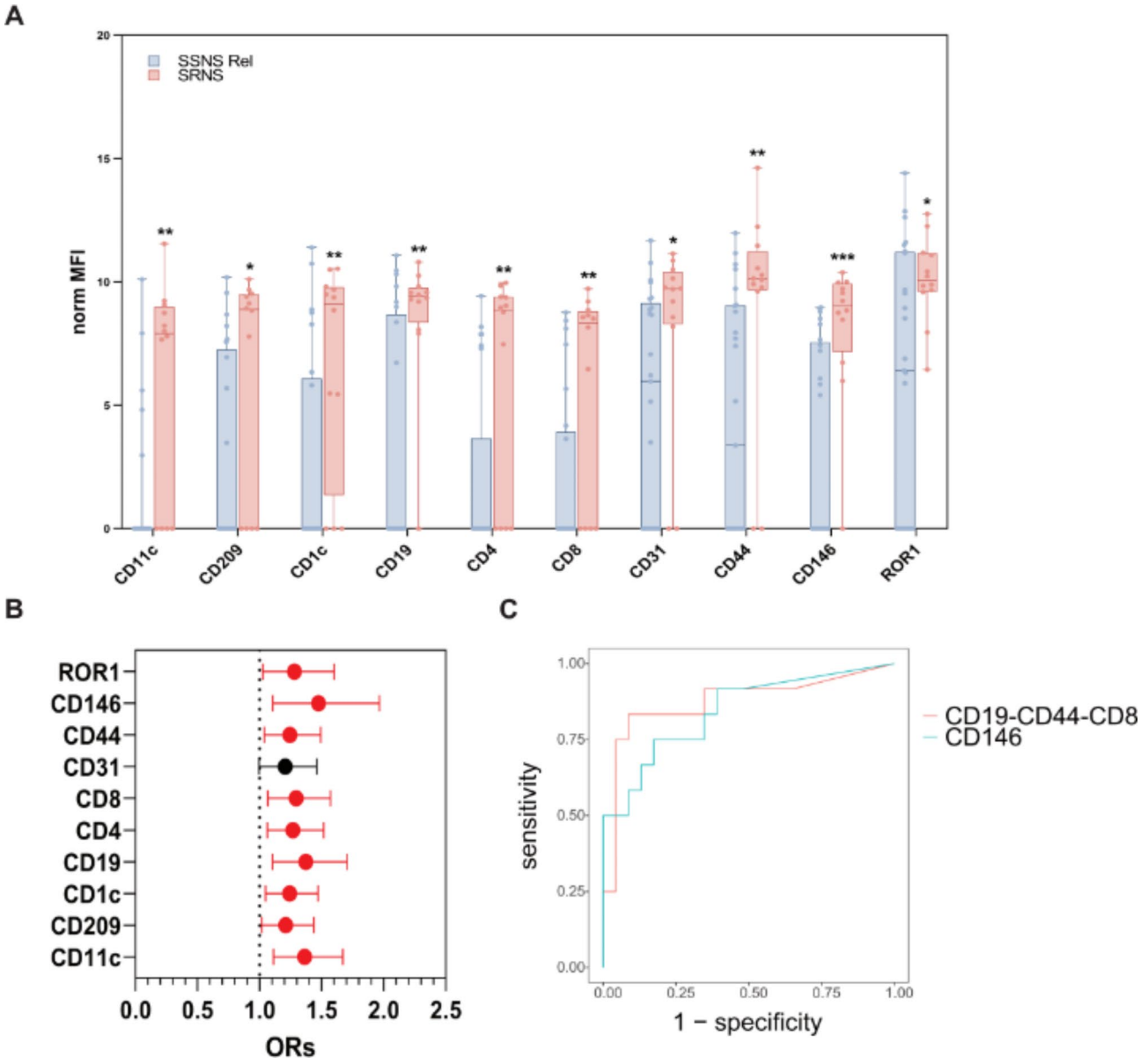

Fig. 5. Expression of uEV markers discriminating steroid-sensitive and steroid-resistant forms of INS. (**A**) Boxplot showing the expression of CD11c, CD209, CD1c, CD19, CD4, CD8, CD31, CD44, CD146, and ROR1 that discriminates between SRNS and SSNS Rel patients. *P < 0.05, **P < 0.01, and ***P < 0.001 vs. SSNS Rel. Non-parametric Mann-Whitney t-test. (**B**) Forest plot of the odds ratio (OR) and its 95% confidence interval for the risk associated with steroid resistance in INS children (OR > 1, positive association; OR < 1, negative association). P < 0.05 is highlighted in red. (**C**) ROC curve analysis of the diagnostic performance of the urinary marker combination (CD19-CD44-CD8, red line) and the single marker (CD146, green line).

differentially expressed markers. This could be potentially ascribed to the difference in the timing of the disease screening; the onset phase represents the initial manifestation of INS, potentially indicating the early pathological condition whereas the relapses happen where the INS condition is already persistent and potentially associated also with ongoing secondary effects. Further, we found that INS patients in the active phase were separated from healthy children based on an exclusive surface signature of 8 markers with a strong overrepresentation of adhesion/endothelial activation markers. Three markers, CD41b (platelets origin), CD105 (endothelial marker), and CD29 (adhesion molecule), showed the best diagnostic score. The CD41b was the principal marker, separating treatment-naïve INS patients at the onset of the disease from controls, thus representing a promising diagnostic biomarker. Interestingly, thromboembolic events represent a possible complication of INS[35]. Moreover, serum endothelial and platelet microparticles were previously described to inversely correlate with kidney function recovery in transplanted patients[23,36]. The EV detected in our samples could potentially derive from the serum since EVs can pass through the membrane pores of the glomerular filtration barrier when kidney damage occurs[19]. Urine EVs can also derive directly from the kidney compartment, where alterations

Markers	AUC	Sensitivity	Specificity	ACC
CD19-CD44-CD8	0.873	0.833	0.913	0.886
CD146	0.844	0.75	0.826	0.8
CD44	0.797	0.833	0.826	0.829
CD19	0.777	0.917	0.696	0.771
CD8	0.75	0.583	0.913	0.8

Table 3. Diagnostic performance of individual, combined uEV markers and proteinuria in steroid sensitivity classification. *AUC* area under curve, *ACC* accuracy.

of the glomerular endothelium have been identified in patients with SSNS in relapse and correlate with poor clinical outcomes[37,38]. Concomitantly, in children with minimal change disease, activation of the integrin CD29/FAK axis was detected in damaged podocytes, suggesting that CD29-enriched EVs could originate from this population[39].

When the EV profile was performed in the same patient using both serum and urine as sources, a better separation of the different stages of INS was achieved. The combination of serum-derived CD146 and urinary-derived CD29 and CD41b reached the best score in separating INS patients in the active phase from healthy children compared to the single markers. While the combination of a unique marker in serum and urine, the CD41b, better distinguished SSNS patients at the onset from CTRL. This approach was also proposed for discriminating pathological states in other diseases[23,40]. The potential impact of EVs in the clinical routine has been widely recognized in cancer diagnosis and prognosis. In this context, EV-enriched miRNAs were shown to be selectively associated with the early detection of tumour appearance[41] as well as poor prognosis and recurrence of highly invasive cancers[42]. Accumulating studies provide strong evidence for the use of EV-protein markers as a diagnostic tool in primary aldosteronism[43], focal segmental glomerulonephritis and steroid-sensitive nephrotic syndrome[44]. Instead, the capability of EV surface antigens to stratify patients according to their renal outcome after kidney transplant was demonstrated by Burrello et al.[23]. A signature of 30 miRNAs was previously described to distinguish INS patients with active proteinuria from patients in clinical remission[45] and correlated with the disease gravity[45]. Similarly, in our experiments, the surface protein markers, CD29, CD41b, and HLA-DR, better correlated with proteinuria levels in our patients' cohort, presenting a disease signature that might potentially anticipate the clinical course of the disease. When each INS subgroup was analyzed, we identified the best classification marker to distinguish the different disease stages in both SRNS and SSNS patients. We found that CD29 was the marker that better discriminates relapse episodes from remission in SSNS patients with an AUC of 0.913, while the SRNS patients were sorted based on the expression of the tetraspanin molecule CD9 (AUC = 1). The expression of integrins was already implicated in the pathogenesis of multiple kidney diseases[46]. Our data corroborates with the recent finding of the group of J. Kennedy, which demonstrated that urinary podocyte-derived large EVs were able to distinguish between relapse and remission phases in children with INS[47]. Additionally, the analysis of biofluids from the same patients in our cohort was able to generate a multi-biomarker combination (CD8 sEVs and CD326 uEVs), which could predict the rate of remission and relapse in SSNS.

We also investigated the role of uEVs surface proteomes in stratifying INS-affected subjects according to steroid sensitivity. Prior investigations identified WT-1 as a marker of urinary exosomes in INS. Despite that, WT-1 expression was ineffective in the prediction of steroid responsiveness in these children[48]. In our study, uEVs were able to separate patients with SSNS from those affected by the SRNS form, based on differences in markers involved in adaptive immune responses and angiogenesis/adhesion-related processes. Among them, the endothelial molecule CD146 better predicts SRNS, with an AUC equal to 0.84. Interestingly, plasma CD146 levels were shown to be progressively increased in early-stage diabetic nephropathy (DN), functioning as an optimal marker in the discrimination of DN severity[49]. Therefore, it is reasonable to suggest that also here increased levels of CD146 in the urine EVs may help discriminate the most severe pathological forms of INS.

However, SSNS and SRNS patients were again better separated by the combination of three markers, CD19, CD8, and CD44, which strongly classified patients based on steroid response. These data highlighted that an unbalanced adaptive immune response activation has an involvement in the progression of the INS disease in patients non-responsive to steroids. The CD19 + B cell levels were recently demonstrated to predict steroid responses in SRNS patients with high sensitivity and acceptable accuracy[50]. Lama G. et al. observed that different immune mechanisms are involved in the pathogenesis of SSNS and SRNS. They found that the higher the CD8 count in children with SRNS, the greater the steroid unresponsiveness[51]. Our data were also in line with a previous study showing the correlation between CD44 expression in kidney biopsies and the higher prevalence of SRNS as well as a negative kidney outcome[52].

Some limitations in this work should be acknowledged. Firstly, the results of our study were limited by the incidence of INS which is classified as a rare disease. Moreover, a longitudinal study on the same patient will be more instrumental in predicting the progression of the disease. However, this study sets the basis to apply the biofluid EV modeling to monitor the ongoing immune-related kidney damage after INS appearance.

In conclusion, our study showed that urinary and serum EV-surface profiles may efficiently separate different forms of childhood INS at different stages of the disease. The urine EVs phenotype mirrored the ongoing immune and endothelial/platelet activation of the disease's active phase. Thus, the EV-surface proteins by reflecting disease-specific features may function as innovative biomarkers in this disease.

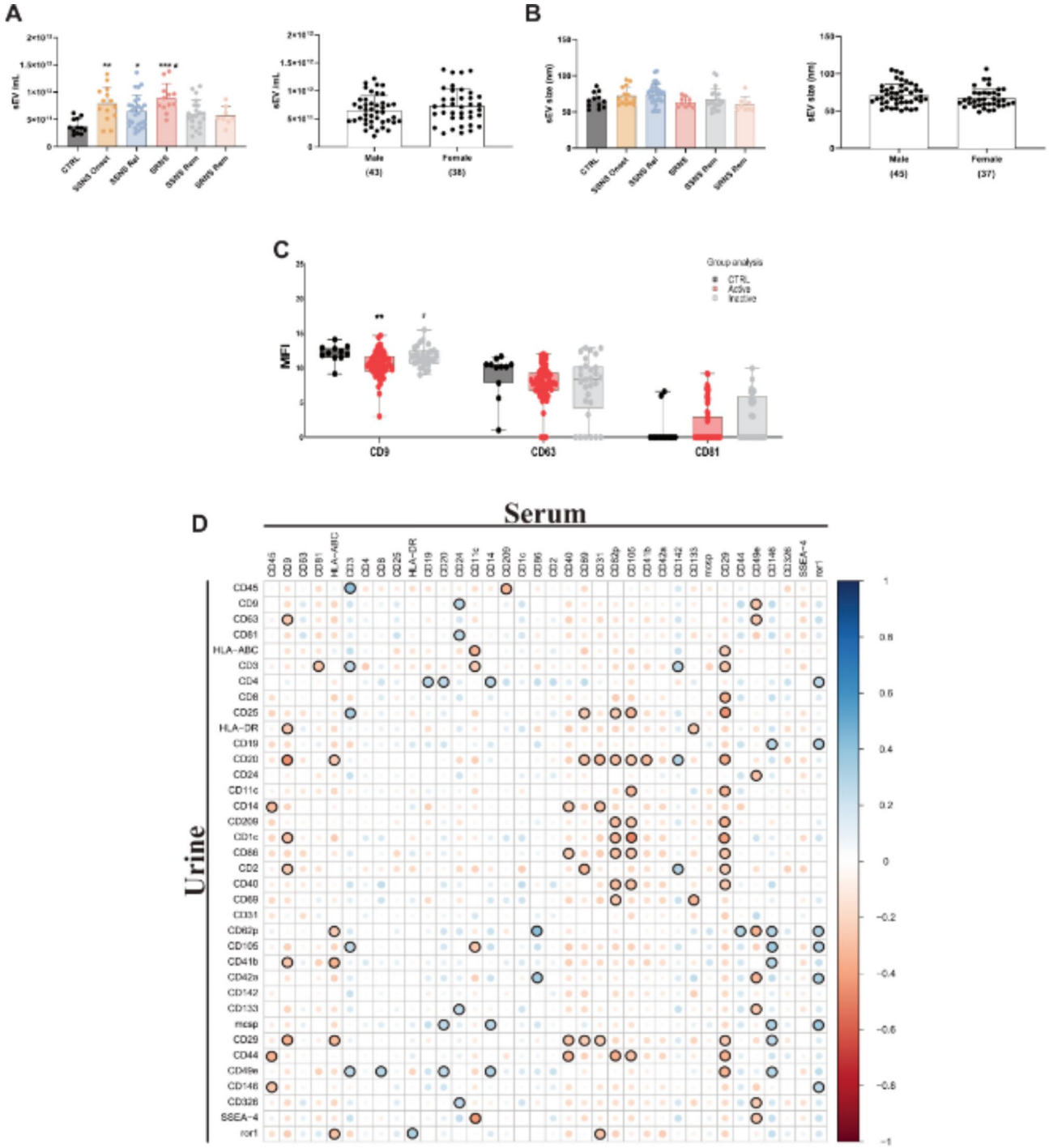

Fig. 6. Correlation analyses of urine and serum-derived markers in the same INS patient. (**A**, **B**) NTA characterization of serum EVs (sEVs) from CTRL and INS patients at different clinical times and separated by gender. Results of sEVs concentration (**A**) and size (**B**) distribution are reported; each dot plot shows the mean ± SD $P < 0.05$, $^{**}P < 0.01$, $^{***}P < 0.001$ vs. CTRL; $\#P < 0.05$ vs. SSNS Rem. One-way ANOVA with Tukey's post-test. (**C**) Flow cytometry characterization of tetraspanins in sEVs from INS patients at different clinical time points, expressed as MFI (CTRL, n = 11; active INS, n = 54; inactive INS, n = 29) $^{**}P < 0.01$ vs. CTRL; $\#P < 0.05$ vs. active INS. Kruskal-Wallis non-parametric with Dunn's post-test. (**D**) Correlation matrix of surface proteins in uEV (Y-axis) and sEVs (X-axis) from the same patient (CTRL, n = 7, and INS group n = 55). R = Pearson correlation coefficient. Negative correlations (red color) and positive correlations (blue color) were highlighted in bold where statistically significant ($P < 0.05$).

s-uEVs Markers	AUC	Sensitivity	Specificity	ACC	Groups
sCD146-uCD29-uCD41b	1	1	1	1	Active vs. CTRL
sCD146	0.8	0.6	1	0.676	
uCD29	0.914	0.867	1	0.89	
uCD41b	0.933	0.867	1	0.89	
sCD41b-uCD41b	1	1	1	1	Onset vs. CTRL
sCD41b	0.964	0.875	1	0.933	
uCD41b	0.911	0.875	1	0.933	
sCD8-uCD326	1	1	1	1	SSNS Rel vs. SSNS Rem
sCD8	0.641	0.533	0.778	0.625	
uCD326	0.97	0.867	1	0.917	

Table 4. Diagnostic performance of uEV and sEV markers in pediatric INS between the different analyzed groups. *AUC* area under curve, *ACC* accuracy.

Data availability

All data generated or analyzed during this study are included in the published article [and its supplementary information files].

Received: 17 April 2024; Accepted: 16 October 2024
Published online: 28 October 2024

References

1. Eddy, A. A. & Symons, J. M. Nephrotic syndrome in childhood. *Lancet*. **362**, 629–639 (2003).
2. Kitsou, K., Askiti, V., Mitsioni, A. & Spoulou, V. The immunopathogenesis of idiopathic nephrotic syndrome: a narrative review of the literature. *Eur. J. Pediatr.* **181**, 1395–1404 (2022).
3. Noone, D. G., Iijima, K. & Parekh, R. Idiopathic nephrotic syndrome in children. *Lancet*. **392**, 61–74 (2018).
4. Tullus, K., Webb, H. & Bagga, A. Management of steroid-resistant nephrotic syndrome in children and adolescents. *Lancet Child. Adolesc. Health*. **2**, 880–890. https://doi.org/10.1016/S2352-4642(18)30283-9 (2018).
5. Hahn, D., Hodson, E. M., Willis, N. S. & Craig, J. C. Corticosteroid therapy for nephrotic syndrome in children. *Cochrane Database Syst Rev* (2015). (2015).
6. Trautmann, A. et al. Long-term outcome of steroid-resistant nephrotic syndrome in children. *J. Am. Soc. Nephrol.* **28**, 3055–3065 (2017).
7. Shah, R., Patel, T. & Freedman, J. E. Circulating Extracellular vesicles in Human Disease. *N. Engl. J. Med.* **379**, 958–966 (2018).
8. El Andaloussi, S., Mäger, I., Breakefield, X. O. & Wood, M. J. A. Extracellular vesicles: biology and emerging therapeutic opportunities. *Nat. Rev. Drug Discovery* 12, 347–357 (2013). (2013).
9. Myette, R. L. & Burger, D. Relapse in steroid-sensitive nephrotic syndrome: are extracellular vesicles the missing link? *Am. J. Physiol. Ren. Physiol.* **321**, F656–F658 (2021).
10. Uddin, J. et al. Extracellular vesicles: the future of therapeutics and drug delivery systems. *Prod. Hosting Elsevier Behalf KeAi*. https://doi.org/10.1016/j.ipha.2024.02.004 (2024).
11. Welsh, J. A. et al. Minimal information for studies of extracellular vesicles (MISEV2023): from basic to advanced approaches. *J. Extracell. Vesicles*. **13**, e12404 (2024).
12. Ståhl, A., lie, Johansson, K., Mossberg, M., Kahn, R. & Karpman, D. Exosomes and microvesicles in normal physiology, pathophysiology, and renal diseases. *Pediatr. Nephrol.* **34**, 11 (2019).
13. Erdbrügger, U. et al. Urinary extracellular vesicles: a position paper by the Urine Task Force of the International Society for Extracellular Vesicles. *J. Extracell. Vesicles*. **10**, e12093 (2021).
14. Takizawa, K. et al. Urinary extracellular vesicles signature for diagnosis of kidney disease. *iScience* **25**(11):105416 (2022).
15. Hogan, M. C. et al. Identification of biomarkers for PKD1 using urinary exosomes. *J. Am. Soc. Nephrol.* **26**, 1661–1670 (2015).
16. Morikawa, Y. et al. Elevated levels of urinary extracellular vesicle fibroblast-specific protein 1 in patients with active crescentic glomerulonephritis. *Nephron*. **141**, 177–187 (2019).
17. Corbetta, S. et al. Urinary exosomes in the diagnosis of Gitelman and Bartter syndromes. *Nephrol. Dialysis Transplantation*. **30**, 621–630 (2015).
18. Zhang, J. et al. Excretion of urine extracellular vesicles bearing markers of activated immune cells and calcium/phosphorus physiology differ between calcium kidney stone formers and non-stone formers. *BMC Nephrol.* **22**, 1–10 (2021).
19. Grange, C., Dalmasso, A., Cortez, J. J., Spokeviciute, B. & Bussolati, B. Exploring the role of urinary extracellular vesicles in kidney physiology, aging, and disease progression. *Am. J. Physiol. Cell. Physiol.* **325**, C1439 (2023).
20. Siddall, E. C. & Radhakrishnan, J. The pathophysiology of edema formation in the nephrotic syndrome. *Kidney Int.* **82**, 635–642 (2012).
21. Barreiro, K. et al. Comparison of urinary extracellular vesicle isolation methods for transcriptomic biomarker research in diabetic kidney disease. *J. Extracell. Vesicles*. **10**, e12038 (2020).
22. Grange C, et al. Urinary Extracellular Vesicles Carrying Klotho Improve the Recovery of Renal Function in an Acute Tubular Injury Model. *Mol Ther.* **28,** 490—502 (2020) [published correction appears in Mol Ther. 2024 Sep 17:S1525-0016(24)00604-X].
23. Burrello, J. et al. Identification of a serum and urine extracellular vesicle signature predicting renal outcome after kidney transplant. *Nephrol. Dialysis Transplantation*. **38**, 764–777 (2023).
24. Ayuko Hoshino, A. et al. Extracellular vesicle and particle biomarkers define multiple human cancers. *Cell.* **182**, 1044–1061. https://doi.org/10.1016/j.cell.2020.07.009 (2020).
25. Mashad, G. M., El, Ibrahim, S. A. E. H. & Abdelnaby, S. A. A. Immunoglobulin G and M levels in childhood nephrotic syndrome: two centers Egyptian study. *Electron. Physician*. **9**, 3728 (2017).
26. Ding, H., Li, L. X., Harris, P. C., Yang, J. & Li, X. Extracellular vesicles and exosomes generated from cystic renal epithelial cells promote cyst growth in autosomal dominant polycystic kidney disease. *Nature Communications 2021 12:1* 12, 1–18 (2021).
27. Noren Hooten, N., Byappanahalli, A. M., Vannoy, M., Omoniyi, V. & Evans, M. K. Influences of age, race, and sex on extracellular vesicle characteristics. *Theranostics*. **12**, 4459–4476 (2022).

28. Lipska-Ziętkiewicz, B. S. Genetic Steroid-Resistant Nephrotic Syndrome Overview. GeneReviews® (2021).
29. Santorelli, L. et al. Diagnostics urinary extracellular vesicle protein profiles discriminate different clinical subgroups of children with idiopathic nephrotic syndrome. https://doi.org/10.3390/diagnostics11030456 (2021).
30. Cereda, C. W. et al. Extracellular vesicle surface markers as a Diagnostic Tool in transient ischemic attacks. https://doi.org/10.1161/STROKEAHA.120.033170 (2021).
31. Castellani, C. et al. Circulating extracellular vesicles as non-invasive biomarker of rejection in heart transplant. *J. Heart Lung Trans.*. **39**, 1136–1148 (2020).
32. Blijdorp, C. J. et al. Comparing approaches to normalize, quantify, and characterize urinary extracellular vesicles. *J. Am. Soc. Nephrol.* **32**, 1210–1226 (2021).
33. Adedeji, A. O. et al. Investigating the value of urine volume, Creatinine, and cystatin C for urinary biomarkers normalization for Drug Development studies. *Int. J. Toxicol.* **38**, 12–22 (2019).
34. Gunasekaran, P. M., Luther, J. M. & Byrd, J. B. For what factors should we normalize urinary extracellular mRNA biomarkers? *Biomol. Detect. Quantif* **17**: 100090 (2019).
35. Eneman, B., Levtchenko, E., van den Heuvel, B., Van Geet, C. & Freson, K. Platelet abnormalities in nephrotic syndrome. *Pediatr. Nephrol.* **31**, 1267–1279 (2016).
36. Martins, S. R. et al. Cell-derived microparticles and Von Willebrand factor in Brazilian renal transplant recipients. *Nephrology*. **24**, 1304–1312 (2019).
37. Bauer, C. et al. Minimal change disease is Associated with endothelial glycocalyx degradation and endothelial activation. *Kidney Int. Rep.* **7**, 797–809 (2022).
38. Royal, V. et al. Ultrastructural characterization of proteinuric patients predicts clinical outcomes. *J. Am. Soc. Nephrol.* **31**, 841–854 (2020).
39. Cara-Fuentes, G. et al. β1-Integrin blockade prevents podocyte injury in experimental models of minimal change disease. *Nefrología* (2022). https://doi.org/10.1016/J.NEFRO.2022.11.004
40. Nagatani, K., Sakashita, E., Endo, H. & Minota, S. A novel multi-biomarker combination predicting relapse from long-term remission after discontinuation of biological drugs in rheumatoid arthritis. *Sci. Rep.* **11**, 20771 (2021).
41. Melo, S. A. et al. Glypican1 identifies cancer exosomes and facilitates early detection of cancer HHS Public Access. *Nature*. **523**, 177–182 (2015).
42. Shi, R. et al. Exosomal levels of miRNA-21 from cerebrospinal fluids associated with poor prognosis and tumor recurrence of glioma patients. *Oncotarget* **6**(29): 26971–81 (2015).
43. Burrello, J. et al. Characterization of circulating Extracellular Vesicle Surface antigens in patients with primary Aldosteronism. *Hypertension*. **78**, 726–737 (2021).
44. Zhou, H. et al. Urinary exosomal Wilms' tumor-1 as a potential biomarker for podocyte injury. *Am. J. Physiol. Ren. Physiol.* **305**, F553 (2013).
45. Chen, T. et al. Increased urinary exosomal microRNAs in children with idiopathic nephrotic syndrome. *EBioMedicine*. **39**, 552–561 (2019).
46. Trevillian, P., Paul, H., Millar, E., Hibberd, A. & Agrez, M. V. αvβ6 integrin expression in diseased and transplanted kidneys. *Kidney Int.* **66**, 1423–1433 (2004).
47. Myette, R. L. et al. Urinary podocyte-derived large extracellular vesicles are increased in paediatric idiopathic nephrotic syndrome. *Nephrol. Dialysis Trans.* **38**, 2089–2091 (2023).
48. Lee, H. K. et al. Urinary exosomal WT1 in childhood nephrotic syndrome. *Pediatr. Nephrol.* **27**, 317–320 (2012).
49. Fan, Y. et al. Expression of endothelial cell Injury marker Cd146 correlates with Disease Severity and predicts the renal outcomes in patients with Diabetic Nephropathy. *Cell. Physiol. Biochem.* **48**, 63–74 (2018).
50. Deng, Y. et al. Peripheral blood lymphocyte subsets in children with nephrotic syndrome: a retrospective analysis. *BMC Nephrol.* **24**, 7 (2023).
51. Lama, G. et al. T-Lymphocyte populations and cytokines in Childhood Nephrotic Syndrome. doi: (2002). https://doi.org/10.1053/ajkd.2002.32769
52. Roca, N. et al. CD44-negative parietal–epithelial cell staining in minimal change disease: association with clinical features, response to corticosteroids and kidney outcome. *Clin. Kidney J.* **15**, 545 (2022).

Acknowledgements

We acknowledge for their support: IMPACTsim S.p.A, ABN (Fondazione bambino nefropatico ONLUS), and Fondazione Nuova Speranza S.p.A ONLUS. The authors wish to thank the Cytofluorimetric facility of the Instituto Nazionale of Genetica Molecolare (INGM) for the cytofluorimetric analysis assistance.

Author contributions

G.C., G.M.,F.C.: Conceptualization; G.C., and A.G.:Data curation and Investigation; G.C., and F.C.: Writing—original draft; G.C. and A.G.: prepared figures; G.C., A.G., S.B., L.B., S.T., C.T., T.N., I.P., A.B., and W.B.: Methodology and Resources; F.C. and G.M.: Supervision, and Funding acquisition. All authors reviewed the manuscript and approved the submitted version.

Funding

Ministero dell'Istruzione, dell'Università e della Ricerca (2022B9WC3F) and IMPACTsim S.p.A funding support (Grant P-0038).

Declarations

Competing interests

The authors declare no competing interests.

Ethics approval and consent to participate

The study was approved by the IRCCS Ca' Granda Institutional Review Board (ID 2633, INSiDe protocol). An informed consensus has been signed by the parent and/or legal guardian of all the children enrolled in the study.

Additional information

Supplementary Information The online version contains supplementary material available at https://doi.org/10.1038/s41598-024-76727-w.

Correspondence and requests for materials should be addressed to F.C.

Reprints and permissions information is available at www.nature.com/reprints.

Publisher's note Springer Nature remains neutral with regard to jurisdictional claims in published maps and institutional affiliations.